Energy Conversion and Management: X 30 (2026) 101770

Contents lists available at ScienceDirect

Energy Conversion and Management: X

journal homepage: www.sciencedirect.com/journal/energy-conversion-and-management-x

Comparison of the design and operation of various fossil-free ferry topologies with a conventional diesel-powered propulsion system – An optimization-based techno-economic-environmental analysis

Chris Drawer *, Luka Bornemann, Martin Kaltschmitt

Institute of Environmental Technology and Energy Economics (IUE), Hamburg University of Technology (TUHH), Eissendorfer Strasse 40, 21073 Hamburg, Germany

ARTICLE INFO

Keywords:
Hydrogen-powered ferry design
Metal hydride storage
Propulsion system optimization
Techno-economic analysis

ABSTRACT

To meet global greenhouse gas (GHG) reduction goals, the shipping sector must also be defossilized. Hydrogen-powered systems could be particularly advantageous for short- and medium-range routes, such as ferries for river or strait crossings. For such applications, metal hydrides offer a promising way to store the hydrogen needed to power the respective ship's propulsion system. In such metal hydrides, hydrogen can be stored safely and without any storage losses under ambient conditions (pressure/temperature). To evaluate the suitability of these metal hydride storage systems as part of a hydrogen-powered propulsion system on ships, the design and operation of ships with metal hydride storage systems must be examined in direct comparison with battery-driven and diesel-powered systems. Therefore, the overarching goal of this paper is based on an optimization-based approach to investigate how a metal hydride system can be operated and designed in a technically and economically viable manner. Furthermore, the environmental performance resulting from such a system is analyzed. The findings show that fuel costs (hydrogen system: 92%, battery system: 85% of total costs) significantly affect the economic viability. Compared to a battery-powered system and a diesel-driven system, the hydrogen-powered system requires the least amount of space. It remains a viable option even with less favorable discharge rates (ranging from 0.03 to 1.0 kW/kWh) of the metal hydride storage system. Thus, if the hydrogen fuel costs decline in the future, such a hydrogen-powered propulsion system for ships could be an alternative to pure battery-based systems. Additionally, the hydrogen-powered system can significantly reduce greenhouse gas emissions compared to a diesel-powered system as long as "green" hydrogen is used.

1. Introduction

The international shipping sector is responsible for roughly 2.5% of global fossil fuel-based CO_2 emissions and therefore clearly contributes to global warming [1]. There are several options to mitigate these greenhouse gas (GHG) emissions. Important levers are direct electrification of the power source, "green" fuels (e.g., methanol, ammonia) produced from renewable energy sources, or "green" hydrogen used directly as an energy carrier [1].

Analogous to ground-bound transport, direct electrification is an option to defossilize, especially smaller vessels with a limited travelling distance. This option relies on electricity stored in rechargeable batteries. However, as with road transport, this technology clearly reaches its limits as weight and distance increase.

"Green" fuels, like biodiesel or bioethanol, will most likely become expensive in the short- and medium-term future due to the a priori limited available potential on the one side and the given demand from various niche markets (e.g., chemical industry, aviation) on the other side [2,3]. Additionally, the so far foreseeable production capacities for these fuels will by far not be sufficient to cover all transportation needs (also including aviation) [4]. Furthermore, air pollution, particularly in populated areas, cannot be avoided entirely.

One other option is to use hydrogen directly without converting it into "green", liquid molecules. Hydrogen conversion products do not pollute the air, and hydrogen can be produced from renewable energy sources via water electrolysis [5,6]. Hydrogen-based fuel cell propulsion systems, therefore, offer one solution to overcome these obstacles, especially for small-scale ships like ferries for river or strait crossings [7,8]. The major problem with such a solution so far is converting the hydrogen required for the respective transportation duty into a form that

* Corresponding author.
E-mail address: chris.drawer@tuhh.de (C. Drawer).

https://doi.org/10.1016/j.ecmx.2026.101770
Received 9 January 2026; Received in revised form 27 February 2026; Accepted 12 March 2026
Available online 18 March 2026

enables intermediate storage with high gravimetric and volumetric energy density. Especially the latter is important for shipping, and here, in particular, for smaller ships/ferries, which cannot provide unlimited space for energy storage(s) [9]. Although liquid hydrogen offers high energy density, its physical properties result in boil-off losses and require complex storage and propulsion facilities. As with renewable liquid fuels, their use is therefore more likely on larger ships traveling longer distances [10,11]. Metal hydride storage systems can be an alternative solution. After the storage reaction (absorption), the hydrogen is stored under ambient conditions; i.e., the storage facility does not need very low temperatures (as, e.g., for liquid hydrogen) or high pressure (as, e.g., for gaseous hydrogen). Beyond that, it has already been shown that, for example, incorporating metal hydride material into a polymer matrix provides high cycle stability [12]. Moreover, the suitability of metal hydrides to react fast enough for efficient hydrogen loading and unloading to cover the energy demand on ships was demonstrated in [13], which investigated discharging rates in depth; but this paper mainly focuses on the thermal system, without analyzing the overall propulsion system. Metal hydride hydrogen storage is characterized by high volumetric energy densities, being up to six times higher compared to modern lithium-ion batteries [14,15], even though the gravimetric density is lower compared to conventional hydrogen storage options [15]; the latter aspect does not lower the promising application possibility for the maritime sector.

Although hydrogen-based fuel cell systems with an integrated metal hydride storage facility offer a promising solution for defossilizing parts of the shipping sector (e.g., small- to medium-sized ferries), there is a lack of studies that deeply investigate the design and operation of the ship propulsion system.

If alternative propulsion systems for ferries / small shipping vessels are investigated, studies focus primarily on pure electric energy systems. For example, in-depth techno-environmental studies of battery ferries were conducted, but without a technical analysis of ferry operations or comparison with a hydrogen-powered ship [16]. A study on the feasibility of retrofitting diesel ships to battery power also revealed that explicit charging schedules are required and that the batteries reduce the usable weight needed [17]. Another example of a ferry transition of about 11 min with a storage capacity of about 320 kWh has been modeled and analyzed [18]. This investigation already shows one major obstacle: the ferry needs to be charged seven times a day. Depending on the ferry schedule, the charging time for such batteries may be too long. As a result, several studies model ferry transitions as a combination of fuel cell and battery propulsion. For example, different ferry routes are compared, among others, for a diesel-operated system and a hydrogen-powered fuel cell system [8]. Here, no operation optimization has been realized, and no battery-only system has been used for comparison. Additionally, no further economic assessment was carried out. Another fuel cell battery hybrid system was investigated without comparison to pure electric or conventional diesel-powered propulsion systems [19]. On larger scales, alternative (liquid) fuels are usually investigated (e.g., [20]). There are already systems that demonstrate the suitability of fuel cell propulsion systems for smaller ships in demonstrator format, but these are generally not optimized in economic or technical terms and do not offer a direct fossil-free comparison with battery vessels, e.g., [21].

Summing up the investigations available so far, many studies focus on selected technologies (mainly technical, rarely economic) for smaller-scale ships or on the use of alternative fuels for larger-scale ships. But several aspects are still missing. First, a balanced and equitable comparison of propulsion systems for a ferry/small-scale ship, including hydrogen fuel-cell propulsion, battery propulsion, and conventional diesel propulsion, which is by far the most widely used technology at this size. Second, the operational optimization, including, e.g., charging when possible within the ferry schedule and not as an externally imposed boundary. Third, the use of metal hydride storages within a hydrogen-powered fuel cell system on a ship. And last, the concurrent analysis of the three mentioned systems on a techno-economic and environmental basis.

This paper aims to address all these points to close the research gaps mentioned. In this work, based on an existing small-scale ferry route, three propulsion systems (hydrogen, pure electricity, and diesel) are optimized in terms of design and operation. The aim is to optimize ferry operations cost-effectively. This paper addresses the research gaps identified by covering the following points.

1. Three different propulsion systems are technically compared with each other under the same conditions, such as an identical timetable and ferry route. This allows for clearly identifying which system dominates in which area (technical or economic), and to determine if there are weaknesses or obstacles to the large-scale implementation of these alternative fossil-free propulsion systems in the ferry sector. Selecting a real ferry route and integrating it specifically into the energy demand profile enables more realistic operating results than idealized routes that are typically used.
2. As a result of the conditions of the existing ferry service, which must be maintained, it is stipulated that all systems under consideration, including their drive systems and (primary) energy storage devices, must be capable of completing the operating day without recharging/refueling. An operational optimization of all three systems is carried out, which, in particular for the battery concept, will enable an equal comparison of all propulsion systems (e.g., in terms of the required storage capacity).
3. A metal hydride storage system is integrated into the hydrogen system under consideration here as a hydrogen storage medium, as an alternative to liquid hydrogen or pressure storage systems that are usually considered. In particular, the flexibility of such a storage system can be modeled concretely for the first time using the route chosen here, taking into account the special conditions that characterize metal hydride storage systems to evaluate their general suitability for such fast-reacting (transport) systems. Consequently, including a metal hydride storage system offers a new (advantageous) perspective on the implementation of fuel cell systems for ferry operations
4. All systems are optimized economically, with the objective function including total annual costs (TAC), enabling a detailed analysis of which cost components dominate. This enables clear recommendations for action regarding the conditions under which such a propulsion system can potentially be operated economically.

From an economic and technical perspective, the issues discussed in this paper can provide valuable insights into the integration of potential alternative propulsion systems for small ships, thereby assisting in answering the question of whether the proposed fossil-free propulsion systems are suitable for the ferry operation considered in this study.

2. Approach

The methodological approach is shown in Fig. 1. Based on different propulsion technologies, a propulsion system for a ferry is designed to meet the energy requirements of a selected ferry route. Technical parameters, such as the power curve representing propulsion and auxiliary power requirements, and economic parameters, such as fuel prices, are specified exogenously. Environmental data, such as specific GHG emissions for various fuels, are also specified exogenously. A mixed-integer linear optimisation approach is used to design selected systems to achieve optimal operating behaviour at the lowest possible total annual costs. Therefore, the system is optimized by determining the optimal operation for each system based on specified upper and lower limits for the respective system components. The optimization leads to techno-economic and environmental results, including storage capacities and volumes, the size of the conversion components, electricity demand, operating costs, and total GHG emissions.

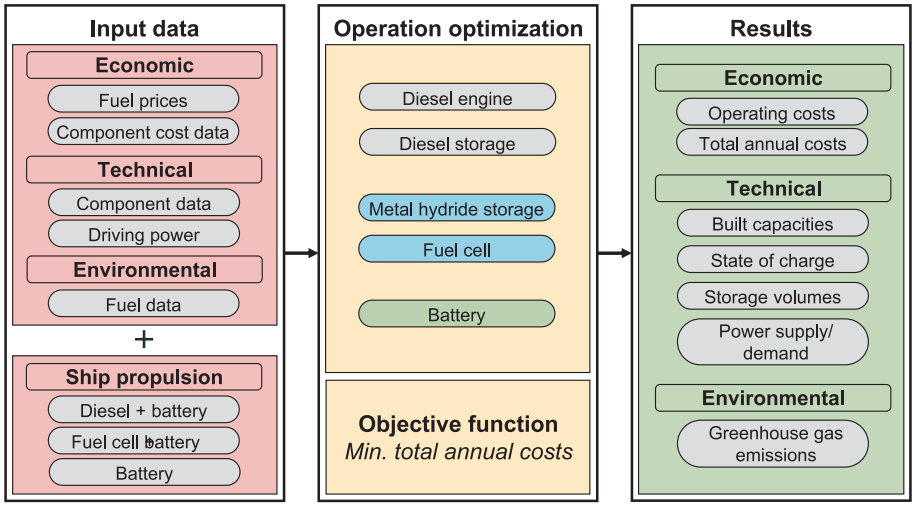

Fig. 1. Overall approach.

2.1. System modelling

The objective function for the optimization system (equation (1)) is defined as the minimum total annual costs (TAC) consisting of daily operating costs ($c_{op,d}$) multiplied by the number of operation days (n_d) per year, annual investment costs ($c_{CAPEX,a,n}$), and the maintenance costs ($c_{main,n}$) for each component ($n \in \mathcal{N}$).

$$\min TAC = n_d c_{op,d} + \sum_{n\in\mathcal{N}} c_{CAPEX,a,n} + \sum_{n\in\mathcal{N}} c_{main,a,n} \tag{1}$$

The daily operating costs (equation (2)) include electricity (*elec*), diesel (*diesel*), and hydrogen (*hydr*) costs per time step (t). The respective costs are summed over the daily operation time period ($t \in T$) multiplied with the time period interval (Δt).

$$c_{op,d} = \Delta t \sum c_{op,elec,t} + c_{op,diesel,t} + c_{op,hydr,t} \tag{2}$$

An annuity factor ($A_{f,n}$) is added for each component (n) to describe the yearly distribution of the CAPEX (capital expenditures) values for the various components ($c_{CAPEX,n}$) over the assumed lifetime; the lifetime of the components differs from one another (equation (3)). It includes an inflation rate (*infl*) and the nominal weighted average cost of capital ($WACC_{nom}$) as well as the deprecation period of the components (d_n) [22] (equation (4)).

$$c_{CAPEX,a,n} = A_{f,n} c_{CAPEX,n} \tag{3}$$

$$A_{f,n} = \frac{\left(\frac{1+WACC_{nom}}{1+infl}\right)\left(\frac{1+WACC_{nom}}{1+infl}\right)^{d_n}}{\left(\frac{1+WACC_{nom}}{1+infl}\right)^{d_n} - 1} \tag{4}$$

The maintenance costs for each component are based on a component-specific maintenance factor. For every timestep (t; i.e., every minute), the sum of demand ($E_{dem,b,t}$) and supply ($E_{sup,b,t}$) for the energy carrier (e.g., electricity, hydrogen) bus ($b \in \mathcal{B}$) has to be zero (equation (5)).

$$E_{sup,b,t} + E_{dem,b,t} = 0 \forall t \in T, \forall b \in \mathcal{B} \tag{5}$$

As part of the optimization process, the optimal combination of possible energy system components is compiled, and their sizes and operating modes are determined cost-optimally.

For certain energy converters, partial-load behavior is assumed, leading to an efficiency curve that depends on load behavior and is implemented analogously to [23].

The full mathematical model is presented in the appendix (chapter 7.1).

2.2. Assessment criteria

The assessment is carried out by analyzing the following parameters derived from the optimization runs for each system layout.

- Size and capacities of the used components.
- State of charge of all storages during one operation day. This involves measuring the fill level of the main storage system (metal hydride storage, battery, and diesel tank) and, if applicable, the auxiliary storage system (battery in the hydrogen-powered and diesel-driven systems).
- Supply and demand of energy through the performance of various components during driving cycles.
- Energy provided by the converters versus energy provided by the storages.
- Total GHG emissions of the respective fuels of all systems during operation. These are based on emission factors for each energy source (electricity, hydrogen, and diesel fuel) and include both direct emissions from operations (where applicable) and upstream emissions caused during production/supply of the fuels (e.g., emissions from production of photovoltaic or wind power plants which are used for electricity supply). Total GHG emissions for each system ($GHG_{tot,t}$) is calculated by multiplying the specific GHG emission factor of the fuel (GHG_{spec}) by the amount of energy which is supplied to the storages for a given period of time ($E_{stor,t}$) (equation (6)). Specific GHG emission factors are listed in Table A4.

$$GHG_{tot,t} = GHG_{spec} E_{stor,t} \tag{6}$$

- Total annual costs for all ferry energy systems consist, on the one hand, of operating costs (i.e., costs for the respective energy source) and, on the other hand, of CAPEX-related costs for the individual components.

3. System description

The evaluated ship energy systems are shown in Fig. 2. A fixed electricity demand consisting of a defined power curve for a predefined ferry route from an electric motor and an additional auxiliary demand is assumed (Fig. 3).

Three different ship propulsion systems are being investigated to meet the specified energy demand curve for the predefined transport

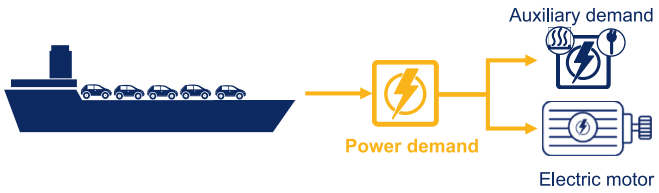

Fig. 2. General system overview.

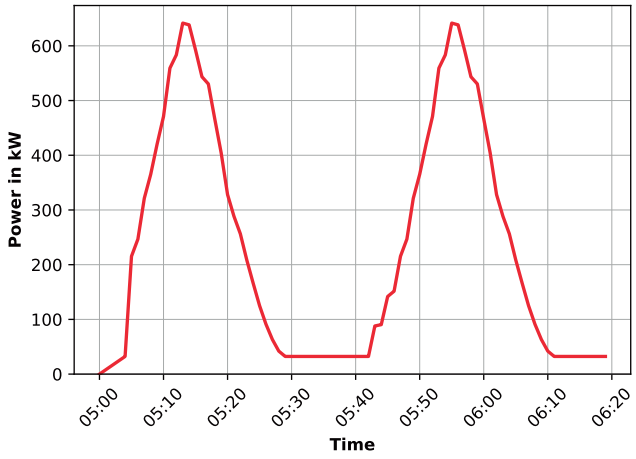

Fig. 3. Power curve ferry route.

route.

- The first system is a conventional diesel engine attached to a generator to provide electricity (i.e., diesel-electric system). It serves as a reference system.
- The second system is based on a polymer electrolyte membrane (PEM) fuel cell, combined with an auxiliary battery to provide electricity. The hydrogen is stored in a metal hydride storage tank (storage material FeTi).
- The third system uses a battery-only system to supply electricity.

The assumptions made for the individual components and the corresponding energy sources (i.e., diesel and hydrogen fuel costs and electricity costs) are decisive for the quantitative classification of the results. In general, degradation effects are neglected in this work, e.g., for the battery and the metal hydride storage system. This study assumes cost data for 2025 for both components and energy. In addition, nominal efficiencies have been specified for the individual components, which will most likely continue to improve in the future as fuel cells and batteries evolve [22]; this evolving trend is neglected here. Furthermore, upstream GHG emissions are included in the emission factors of the individual systems, deviating from some regulatory definitions, e.g., [24], to reflect the actual emissions of the individual propulsion systems.

Cost data for the fuels and other economic data are given in Table A3. All techno-economic data for the components are provided in Table A2.

3.1. System definition

The power demand reflects the energy required to cross the River Elbe in Northern Germany, an exemplary ferry route. The route is selected in particular to evaluate how the drive systems under investigation behave in the context of a small-scale ferry connection, which involves high frequency with short distances and frequent acceleration and braking. The power curve is based on measured speed profile data for a selected ship [25]. A crossing takes 28 min, followed by a 14 min stop at the port for loading and unloading of cars and passengers. Then the cycle begins again. It is assumed that a certain amount of auxiliary power is continuously required at each port [10]; hence, the power demand does not drop to 0 even during stops. Exceptions are before the first trip of the day and at the end of the day. The power demand curve for the first two cycles (i.e., one cycle is one crossing) of a day is shown in Fig. 3.

The driving cycle is repeated throughout the day from 5 am to 10.30 pm, always following the same pattern. The power curve is available at 1 min resolution (i.e., the optimization time interval is 1 min).

Optimization requires suitable limits within which the components can be optimized in terms of their design. The required upper and lower limits for each propulsion system are summarized in Table 1. The upper limits are set after preliminary investigations in which the maximum capacities expected to be required were analyzed. Technical details of all components that are included in the different systems are provided in Table A2.

3.1.1. Hydrogen-powered system

Within the hydrogen propulsion system, a fuel cell as the primary energy converter, a hydrogen storage system, and a battery are included. Fig. 4 shows the layout of such a propulsion system. Hydrogen is stored in a metal hydride storage tank. The metal hydride storage system is based on the material FeTi. The material specification is relevant in the context of the energy system because, on the one hand, the temperature level must be suitable for the PEM fuel cell used here. On the other hand, the enthalpy difference required to operate the metal hydride storage system must be defined. The two storage systems differ in their limitations:

- The metal hydride storage can only be filled once, at the start of the day. This energy is then released throughout the day, resulting in the storage system being completely empty by the end of the day.
- The battery storage cannot be charged externally, i.e., on land, but only internally via the fuel cell. Unlike the metal hydride storage, it must also have the same fill level at the end of the day as at the beginning.

These assumptions are intended to address the different functions of the storage systems: the metal hydride storage is the main energy supplier for the propulsion system, while the battery can provide support, for example, to bridge load peaks or to compensate for the unfavorable partial-load efficiency of the fuel cells.

3.1.2. Battery-only system

Another fossil-free alternative for ship propulsion is a pure battery system. The respective system layout is shown in Fig. 5. The electrical energy required to power the ship is drawn directly from the battery, which is the only component within the ship's propulsion system under consideration. As in the hydrogen-powered system, the battery is not intended to be recharged during the day, but can be fully charged once during the night / at the beginning of the operating day, similar to a metal hydride storage system, and then release this energy throughout the day. The battery must therefore be designed sufficiently to store enough energy for a single day's cycles, assuming that it can be completely recharged during the night.

Table 1
Capacity ranges of available components for optimization for all system layouts.

Component / Capacity range	Diesel	Hydrogen	Battery
Diesel storage	0 – 30 MWh	–	–
Diesel engine	0 – 1 MW	–	–
Battery	0 – 500 kWh	0 – 500 kWh	0 – 15 MWh
Metal hydride storage	–	0 – 30 MWh	–
Fuel cell	–	0 – 1 MW	–

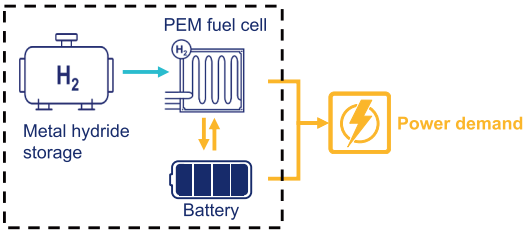

Fig. 4. Layout of the hydrogen-powered system (yellow: electricity, light blue: hydrogen). (For interpretation of the references to colour in this figure legend, the reader is referred to the web version of this article.)

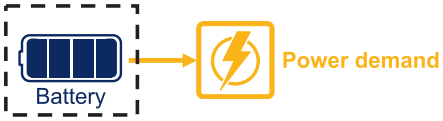

Fig. 5. Layout of the battery-only system (yellow: electricity). (For interpretation of the references to colour in this figure legend, the reader is referred to the web version of this article.)

3.1.3. Diesel-powered system

The diesel-powered propulsion system for the investigated ferry comprises a diesel tank, a diesel engine for power generation, and a battery to cover peak loads (Fig. 6). This concept is becoming increasingly common in modern ships [26,27]. The fuel is stored within a conventional diesel storage tank. Since state-of-the-art technology is assumed, peak loads are buffered by a small battery, enabling power to be supplied from the battery or the generator. The generator is included in the modeling and in the term “diesel engine” below. The battery can only be charged via the diesel engine and cannot be connected to an external power grid (analogous to the hydrogen-powered concept). The diesel tank can be filled up completely at the start of the day and release energy throughout the day. Similar to the hydrogen-powered system, the peak-shaving battery must have the same amount of energy at the start and end of the day and should support load smoothing, as the diesel engine, like the fuel cell, has a non-linear efficiency curve.

3.2. Analyzed cases

Two different groups of cases are defined. First, base cases for each system layout, and second, modifications of selected parameters across three parameter variations, resulting in modified systems to analyze selected effects.

3.2.1. Base cases

For the three investigated propulsion systems, different limitations must be met to ensure that each technology can be examined in detail. The main difference between the various system configurations addresses the limitation of the energy supplied via the battery. For all systems, recharging at the port stays is not assumed (i.e., each system is completely charged at the start of the operation period). Thus, the battery within the battery system must be designed to enable the ferry to operate for an entire day without recharging from an external energy source (e.g., at port stops). This prohibition on recharging should enable comparability between hydrogen and diesel ships, which would not be possible with permitted reloading. This also eliminates the need for further infrastructure development, such as the installation of fast charging stations at both port facilities, which would be required in addition to providing the infrastructure for the primary energy sources for each system. In diesel- and hydrogen-powered systems, the battery may supply up to 10% of the daily energy requirement. This order of magnitude corresponds to the typical proportions of a hybrid ship of the size examined [28–30]. For hydrogen- and diesel-powered vessels, the battery charge level at the start of the day must match that at the end of the day to ensure the battery is integrated, primarily to smooth the power curve. The system's layout details are shown in Table 2 and described below. All cost data (e.g., fuel prices) and details for supporting points used to linearize non-linear efficiency curves are displayed in Table A1.

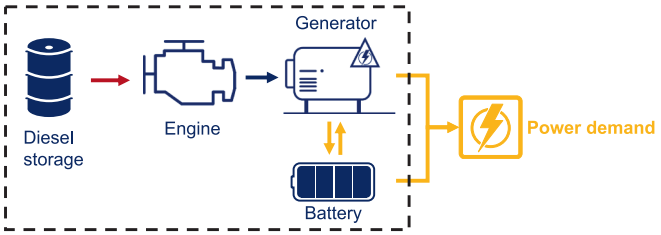

Fig. 6. Layout of the diesel-powered system (yellow: electricity, red: diesel, dark blue: mechanical energy). (For interpretation of the references to colour in this figure legend, the reader is referred to the web version of this article.)

3.2.2. Parameter variation

Several assumptions made in the base case definitions might significantly influence the results of the various propulsion systems. This includes, e.g., the availability of land-based power during port stays for loading and unloading; this could be a viable option with the emergence of fast battery charging [33]. Additionally, the ship's auxiliary power requirements could also be covered by shore power.

Charging and discharging rates are important parameters for metal hydride storage systems. Since the loading and unloading of metal hydrides is generally slower than that of conventional hydrogen storage options [9], this factor may be particularly important for the application scenario assumed here.

Finally, the development of fuel prices could have a significant impact on system costs. The data used in this study are based on the situation in 2025 and are naturally subject to change.

As a result of these aspects, the parameters discussed below are varied independently of each other.

- In the first parameter variation, it is assumed that the ship will be connected directly to the power grid when it is in the harbor. This allows the battery to be charged and/or shore power to be used to meet the ship's power requirements directly. For the change in the state of (dis)charge pattern and the potentially changed volume of storage, as well as for the total annual costs of the systems, the results of this parameter variation are compared with those of the base cases defined in chapter 3.2.1.
- In a second parameter variation, different maximum discharge rates are assumed to analyze how they could affect total annual costs and the capacity of the corresponding metal hydride storage.
- In a third parameter variation, the costs for the respective energy sources (i.e., hydrogen, electricity, and diesel fuel) are varied to determine their influence on the total annual costs.

Table 2
Main assumptions for all systems (SOC State of charge).

System / Limitation	Battery SOC	Battery energy supply	References
Diesel-powered system	Start = End	≤ 10% of total energy demand	based on [31]
Hydrogen-powered system	Start = End	≤ 10% of total energy demand	based on [32]
Battery-only system	No limitation	No limitation	–

4. Results and discussion

The results are analyzed for the base cases (chapter 4.1) and for the parameter variations (chapter 4.2).

4.1. Base cases

The results for the base layouts are shown below. Depending on the results, three time periods are analyzed: one year, one day, or one cycle (i.e., one river crossing).

4.1.1. Installed capacities

All built capacities for the three systems are shown in Fig. 7. The hydrogen-/diesel-powered system comprises an energy conversion technology (a fuel cell/diesel engine) and two storage components (a battery and a metal hydride storage/battery, and a diesel tank). The pure battery system has only the battery as an energy storage.

Based on the optimization, the hydrogen system is equipped with a fuel cell of about 0.58 MW, while the metal hydride storage system has a storage capacity of 9.79 MWh. The size of the hydrogen-powered energy converter and storage system is roughly comparable to that of the diesel-powered system, which, however, shows a slightly smaller storage capacity (for diesel fuel). In contrast, the pure battery-operated system, with the battery as the only component, has a storage capacity of 4.39 MWh. The clearly lower storage capacity of the battery-only system compared to the hydrogen and diesel-powered systems indicates that the hydrogen and diesel-powered systems are most likely significantly less energy efficient and thus require significantly more “input energy.”.

The difference in required storage capacity, combined with the specific volumetric energy density, can be illustrated by the total storage volume required for each ship topology.

Although batteries require the least storage capacity in terms of stored energy, they also have the lowest specific energy density (compared to hydrogen stored in metal hydrides and diesel fuel) and require a storage volume of ca. 9 m^3 without recharging during the day. Only roughly one-third of this storage volume is needed for the hydrogen-powered system, as the metal hydride storage shows a much higher specific volumetric energy density and thus needs less space. The battery integrated into this concept has a small storage capacity and, therefore, a small volume. Compared with a conventional diesel-powered system, the required storage volume is less than 1 m^3, as diesel has the highest specific volumetric energy density of the three storage types.

These results demonstrate an advantage of the hydrogen-powered system over the battery-only system, as volume and space requirements on ships are important factors, even though the total energy stored in battery systems may be lower.

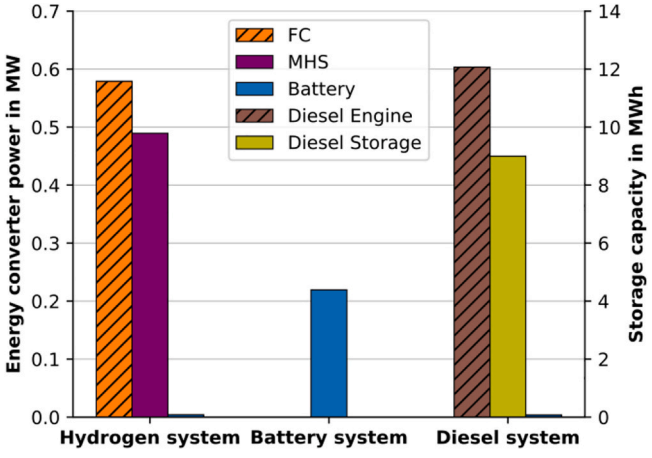

Fig. 7. Component capacities for all systems (FC Fuel cell, MHS Metal hydride storage; size of the conversion components on the left vertical axis, size of the storage components on the right vertical axis).

4.1.2. State of charge

Fig. 8 shows the state of charge for all systems, along with the corresponding storage capacities for one day of operation. Since the systems are optimized for minimal annual costs, the primary storage units (i.e., the metal hydride storage within the hydrogen-powered system), which cannot be recharged during the day, are designed to continuously supply energy from early morning until they are completely depleted at the end of the operation day. For the hydrogen and diesel-powered system, the state of charge of the batteries indicates that they are only supporting the main energy supplier for peak energy shaving. In the hydrogen-powered system, the pattern is very regular, suggesting that the battery is used for regular stops and possibly also for peak energy demands at the beginning of each crossing cycle. The battery capacity is far from being fully utilized (in both the hydrogen- and diesel-powered system), and the battery usually operates between 0 and 30%; i.e., the full capacity of 100% is not being utilized. This can be explained by the charging and discharging rates determined by the storage capacity; i.e., a fixed charging and discharging rate, expressed as power per storage capacity, is assumed. If a high discharging rate is required at certain time periods (e.g., when increasing the power at the start of the driving cycle), a high discharging rate is required, resulting in a high storage capacity. Similar behavior can be observed in the diesel-powered system. In accordance with the material specifications of the metal hydride storage material, the storage limits are assumed to be 10% and 90%, respectively.

Furthermore, each river crossing involves the same driving cycle, with slight deviations in the first and last cycles, which start and end with an energy requirement of 0 (Fig. 3). The daily fluctuation in the battery level observed in the state of charge curves of the hydrogen and diesel-powered systems (Fig. 8) can be explained by minimal deviations from the calculated optimum within the scope of optimization, which accumulate over the course of the day but do not significantly affect the results with regard to the state of charge.

4.1.3. Operation

Fig. 9 shows the energy demand for all propulsion systems during one river crossing (driving cycle) and the supply required to meet that demand.

The hydrogen-powered system (Fig. 9, top) shows that the ship's energy requirements are met by a combination of energy provision from

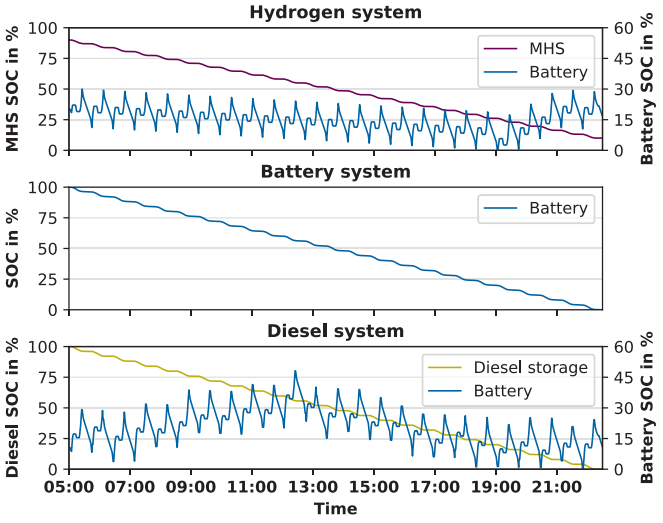

Fig. 8. State of charge (SOC) of the respective storages for all systems (MHS Metal hydride storage).

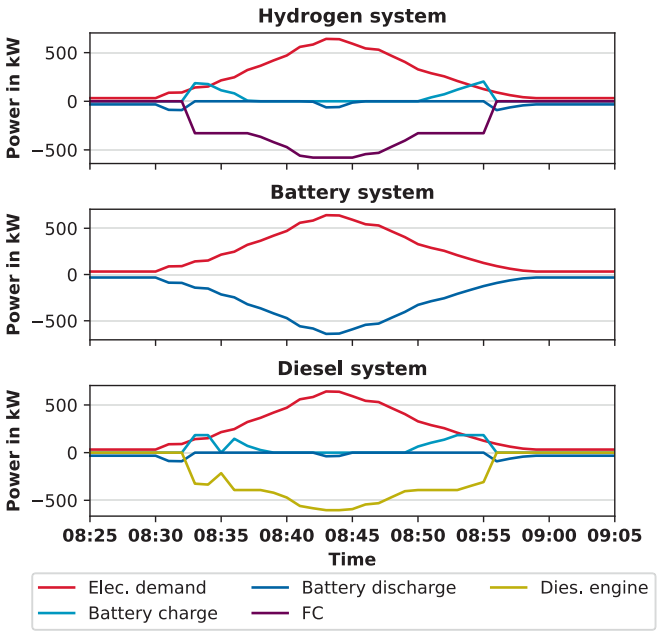

Fig. 9. Operation energy balance of all systems for one driving cycle (positive values are energy demands and negative values the corresponding supply; Elec. Electricity, Dies. Diesel, FC Fuel cell).

the fuel cell and from the battery. The fuel cell is ramped up directly to a load of 321 kW, more than needed to meet the power demand, so the battery can also be charged. After a constant-power period, the fuel cell power increases further to a maximum of 566 kW. The remaining energy is supplied by the battery, with around 75 kW at peak power. A similar behavior is observed during the ramp-down phase of the fuel cell: the system tries to keep the fuel cell power constant as long as possible, using the additional power generated to charge the battery. The small power demand during the port stay is fully covered by the battery, with a capacity of 32 kW. This behavior indicates that the fuel cell is ramped up and down as quickly as possible to avoid load ranges that are unfavorable to efficiency. The resulting excess electricity can be fed into the battery. The desired effect of load smoothing by the battery, inferred from the state-of-charge pattern, can thus be confirmed.

In the battery-only system, a priori, the power can only be supplied via the battery. However, load smoothing is not necessary in this system, as no load-dependent efficiency is assumed for the battery storage.

The diesel-powered system behaves similarly to the hydrogen-powered system. The battery covers the peak value at the middle of the driving cycle, so that the diesel engine's power output does not exceed 574 kW. This is due to differences in efficiency assumptions for the diesel engine.

4.1.4. Supplied energy

Fig. 10 shows how much of the primary energy used in one year (i.e., the energy fed into the storage system) can be used to cover the energy demand after conversion or withdrawal from the respective energy converters (or from the storage system in the case of the battery system).

The energy supplied by the battery can be used immediately to meet power requirements, resulting in "only" charging and discharging losses.

In contrast, the metal hydride hydrogen storage, part of the hydrogen-powered system, has an energy content of 2.9 GWh/a, exceeding the battery's by more than 1.6 times. The comparison of the energy released from the metal hydride storage facility and the electrical energy ultimately supplied from the fuel cell shows a considerable loss of energy (i.e., a loss of "usable" energy). The additional thermal energy released by the fuel cell can be used to provide more than 85% of the activation energy required for the metal hydride storage tank during

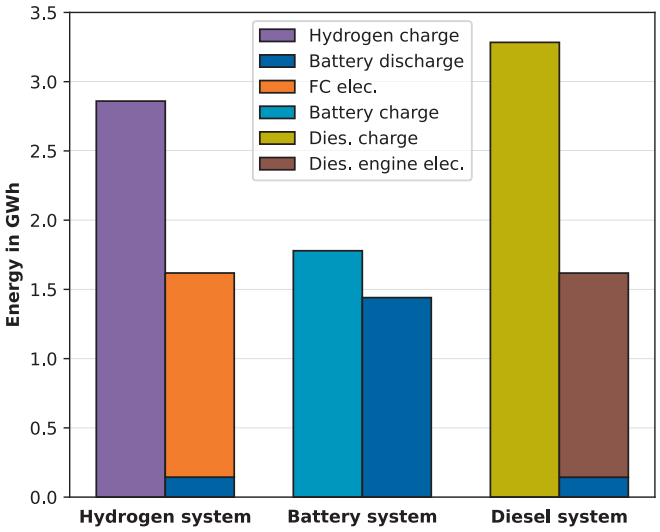

Fig. 10. Available energy (left bars) and supplied usable energy (right bars) within operation for all systems over one year (Dies. Diesel, FC Fuel cell, elec. Electricity).

hydrogen discharge.

The diesel-powered system accounts for the largest share of "primary ship energy". At around 3.3 GWh/a, the energy released by the diesel tank is more than 1.8 times that of the battery system. The relatively low electrical efficiency of the diesel engine necessitates storing a large amount of energy as diesel fuel. The reason for these high losses is that a considerable amount of energy is converted into excess heat, which, unlike in the hydrogen-powered system, cannot be used (i.e., there are no heat consumers).

When considering the ship propulsion system alone, without accounting for prior conversion chains, the battery-only system achieves the highest electrical efficiency. Although the losses are significantly higher in the hydrogen-powered system, a high proportion of waste heat can be utilized, at least by matching the temperatures of the metal hydride storage and the fuel cell.

4.1.5. Greenhouse gas emissions

The greenhouse gas (GHG) emissions, caused by the fuel (combination of production and use) within one operational year, are displayed in Fig. 11.

GHG emissions from hydrogen are solely due to the energy required for its production, as no GHG emissions are released during combustion/use. Assuming that the electricity used for hydrogen production comes

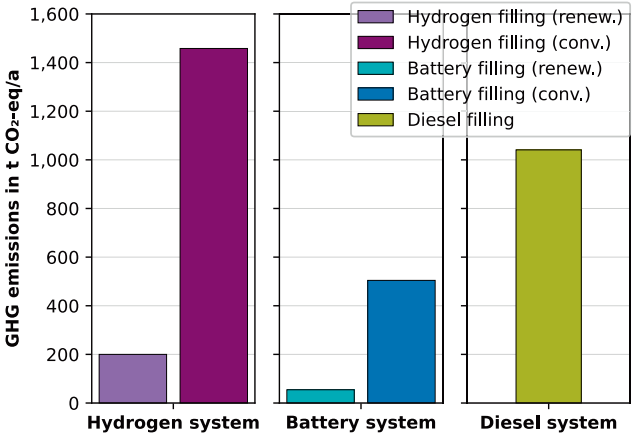

Fig. 11. Greenhouse gas (GHG) emissions for all systems over a year.

from renewable sources, the GHG emissions within the hydrogen system sum to 200 t CO_2-eq/a. These include, in addition to upstream emissions from the necessary electricity generation, ca. 4% of the emissions from electrolyzer production [34]. This approach differs from the European Union's regulatory framework, which considers "green" electricity for hydrogen production to have an emission factor of 0 g CO_2-eq/kWh [24]. In this work, however, the actual emissions should be taken into account. When using the German electricity mix (2025), GHG emissions actually exceed those of the diesel-powered system, at around 1,458 t CO_2-eq/a.

Within the framework of a battery-only system, GHG emissions are released only during electricity production; no GHG are emitted during operation. Based on the current electricity mix, the GHG emissions are around 504 t CO_2-eq/a. These mainly include emissions from the combustion of fossil fuels, which are part of the electricity mix. Assuming a renewable electricity mix, the battery-only propulsion system can achieve a significant reduction to around 55 t CO_2–eq/a.

The GHG emissions of the diesel-powered system are almost entirely driven by diesel fuel combustion. Due to the overall high GHG emissions (1,043 t CO_2-eq/a) of the diesel-powered system, production of the fuel plays with ca. 17% only a less significant role compared to the supply of electricity and hydrogen within the other systems [35].

Even though the GHG emissions from using hydrogen within the hydrogen-powered system exceed those from the battery used within the battery-only system, assuming that renewable electricity is used, the comparison with the reference system shows that the contribution of diesel to the GHG emissions is much higher; i.e., switching from diesel to hydrogen, the GHG emissions can be reduced by roughly 80%.

4.1.6. Total annual costs

The total annual costs (TAC) of the three systems examined are shown in Fig. 12. These costs include the annualized investment and maintenance costs, as well as the annual operating costs. The total annual costs of all systems are clearly dominated by fuel costs, accounting for between 85% (battery-only system) and 97% (diesel-powered system) of the total costs.

The hydrogen-powered system shows the highest costs by far at 0.62 Mio. €/a, because hydrogen currently has the highest specific provision costs of the three fuel types (hydrogen, electricity, diesel). Despite the high storage capacity of metal hydride storage and the associated CAPEX costs, this is hardly significant in terms of total annual costs (due to the high cost of the hydrogen used). After hydrogen costs, fuel cell investment costs account for the largest share of the hydrogen-powered system's total annual costs, at 4%.

At 0.34 Mio. €, the battery-only system has significantly lower total annual costs, benefiting in particular from the fact that the purchased electricity can be used to cover the ship's energy requirements with almost no losses, even though the specific costs are higher than those of diesel fuel. The battery's CAPEX accounts for 12% of total annual costs.

The lowest annual costs are incurred by the diesel system, at around 0.22 Mio. €. The very low specific diesel costs are the reason for this, even though the diesel system has the worst efficiency of all the systems considered (i.e., the use of fuel energy in the tank relative to the final provision of energy from the engine).

Given the clearly dominant fuel costs across all systems, the key lever for economic optimization is the reduction of fuel supply costs.

4.2. Parameter variation

Three additional aspects are included separately within the parameter variation: allowing charging of the batteries at the harbor stops, changing the maximum discharge rate for the metal hydride storage tank, and changing the energy carrier costs.

The changed conditions within the three parameter variations lead to some new systems/system configurations. This can lead to changes in all results that are analogous to the base cases. However, a significant change occurs only in selected results from the three parameter variations, which will be discussed in detail below.

4.2.1. Port shore power

Allowing batteries to be charged with shore power results in significant changes, particularly in the state of charge of the storage systems over the course of the day (Fig. 13). In addition, changes can be observed for the hydrogen-powered system and the battery-only system in terms of total annual costs and the resulting (significantly reduced) storage capacities (Fig. 14 and Fig. 15).

The ability to charge batteries via shore power shows a significantly different discharge behavior.

For the battery-only system, at every stay at the harbors, the battery can be charged by about 50%-pt. Thus, under these conditions, the required storage capacity might be significantly reduced.

The charging pattern of the battery within the hydrogen-powered

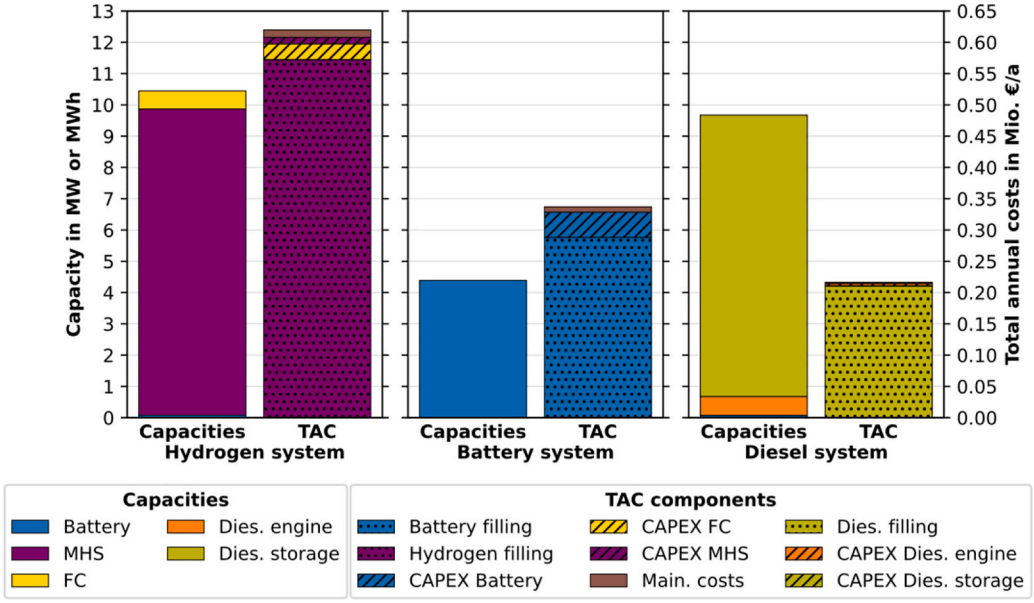

Fig. 12. Total annual costs (TAC) for all systems (MHS Metal hydride storage, FC Fuel cell, Dies. Diesel, Main. Maintenance).

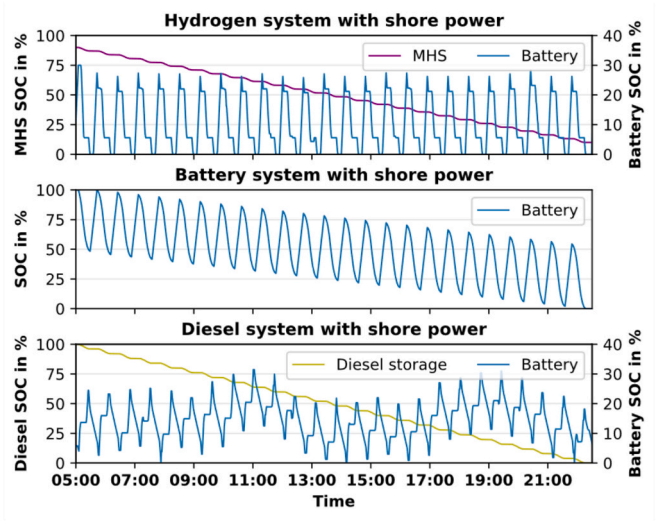

Fig. 13. State of charge (SOC) of the respective storages for all systems with additional shore power (MHS Metal hydride storage).

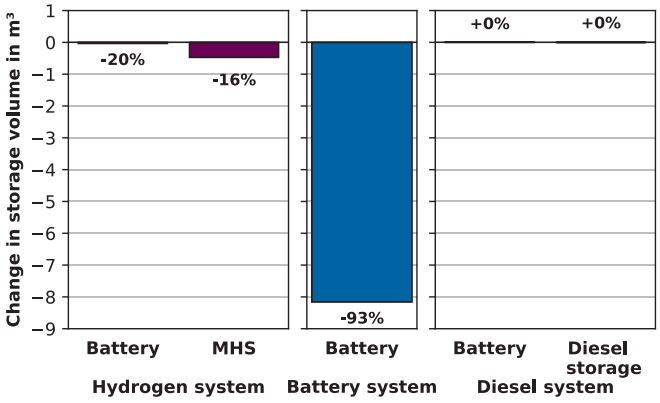

Fig. 14. Storage volume reduction with shore power, all systems (MHS Metal hydride storage).

system also shows that it is regularly charged via shore power. While the reduction in size of the ship's battery and thus the reduction in CAPEX is likely to be a decisive factor in the use of shore power for the battery-only system, most likely within the hydrogen-powered systems the focus is on substituting the more expensive energy source hydrogen with (cheaper) electricity in the form of external electricity supply during the stay within the harbor.

In the diesel-powered system, on the other hand, land-based charging is not an option. Due to diesel's lower cost as an energy source, this is not advantageous from an economic standpoint.

The extent to which a possible change in storage capacity affects the required volume on board is shown in Fig. 14. The largest reduction in storage capacity due to this port recharging option is observed in the battery-only system. Here, the installed battery capacity can be reduced by about 93% compared to the base case. Smaller changes occur within the hydrogen-powered system, where the potentially more expensive hydrogen storage is reduced by 16%. The battery storage capacity itself is only slightly decreased (in absolute terms), suggesting that the system's lower storage capacity is compensated for by direct grid power consumption at ports. This is because operating with hydrogen is more expensive than with direct electricity / battery power, with clearly lower conversion losses and lower specific costs. No change in the diesel system has been observed. This is presumably due to the significantly lower specific costs of diesel fuel, which make it economically unviable to purchase more expensive electricity from the external power grid. These changes in volume and capacity (Fig. 14) initially indicate an advantage of the battery-only system over the hydrogen-powered system.

The effects on state-of-charge and volume change can be explained by analyzing the total annual costs of the systems (Fig. 15) when shore power is included. The main differences can be observed within the battery-only system. The total annual costs decrease by ca. 0.5% due to a significantly smaller battery being installed, as shown in comparison with the overall base case capacities (only the battery within the battery system). The operating costs are the same, as the electricity costs are the same for regular charging at the harbors and for (initial) battery charging before the start of the day. More extended changes can be observed within the hydrogen-powered system; fewer (storage) capacities are built, resulting in a total annual cost reduction of around 8%. No changes were observed in the diesel system, as the shore power option is not used.

In summary, despite the possibility of using shore power in harbors,

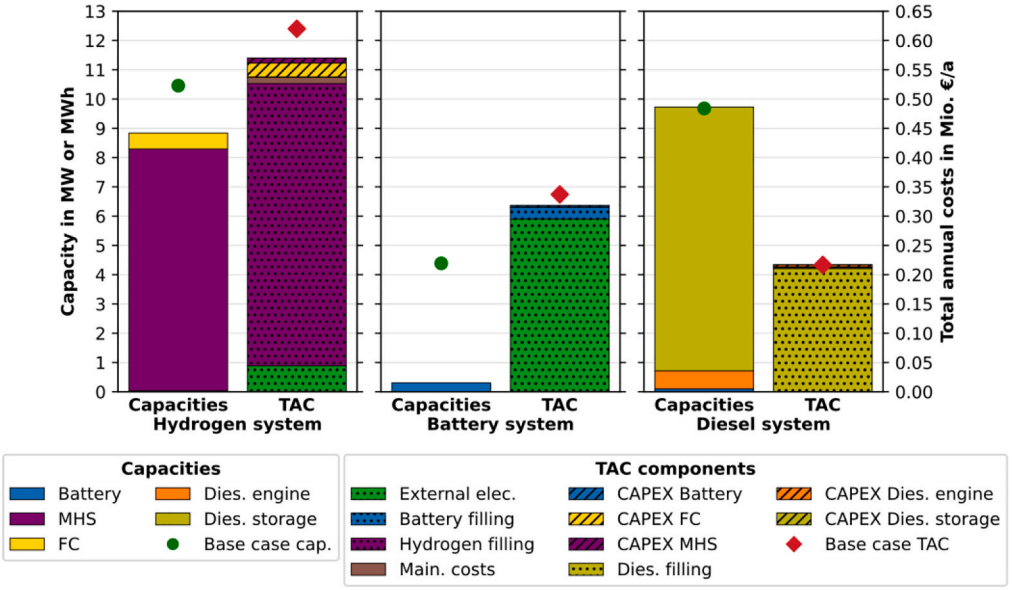

Fig. 15. Total annual costs (TAC) for all systems with shore power (MHS Metal hydride storage, FC Fuel cell, cap. Capacities, elec. Electricity, Dies. Diesel, Main. Maintenance).

total annual costs for the battery system change only slightly, whereas installed capacity changes significantly. Storage capacities, especially for battery-only systems, can be reduced considerably. However, the biggest changes in total annual costs are observed with the hydrogen-powered system due to the relatively high hydrogen fuel costs.

4.2.2. Change in maximum discharge rate

By varying the maximum discharge rate, it is to be examined, on the one hand, to what extent the metal hydride storage capacity changes and, on the other hand, what influence this changing storage capacity has on total annual costs through CAPEX changes.

Within the base case of the hydrogen system, the maximum discharge rate of the metal hydride storage is set to 0.3 kW/kWh. To evaluate the influence on the optimization, this value is modified. As shown in Fig. 16, an increase in the maximum discharge rate (i.e., potentially speeding up discharge) does not affect the built hydrogen capacity and therefore has no effect on the total annual costs. Reducing the maximum discharge rate to below 0.1 kW/kWh, and even to a significantly lower level below 0.05 kW/kWh, increases the installed storage capacity, as the discharge rate is related to the installed capacity. This is associated with an increase in total annual costs. However, as operating costs account for the majority of total annual costs, even at the lowest achievable discharge rate of 0.03 kW/kWh, total annual costs are only 9% higher than in the base case. In summary, the discharge rate used in the base case provides sufficient flexibility for upward and downward fluctuations without significantly affecting the results.

4.2.3. Change of energy carrier costs

Evaluating the total annual costs for all systems, it is clear that fuel costs significantly influence the economic viability of each system. Based on this, a parameter variation is carried out as follows, reducing or increasing fuel or electricity costs by 25% and 50% to evaluate the impact on the TAC. Fig. 17 shows the results for all systems.

Since energy costs account for between 85% and 97% of total costs across all systems, this increase or reduction is reflected almost equally in total annual costs. Varying the energy carrier costs only moderately (+/- 25%) shows already a significant change in total annual costs. The hydrogen system will see the largest increase in absolute terms, rising from 0.62 Mio. € to 0.77 Mio. €, with a 25% increase in hydrogen costs. As a result of the fact that the diesel-powered ship has the lowest TAC in the base case, the changes caused by the variation in energy costs are also the lowest in absolute terms. With a 25% increase in diesel costs, the TAC increases from 0.22 Mio. € to 0.27 Mio. €.

Only when the fuel costs decrease extremely, e.g., by 50%, the hydrogen system might be economically competitive with the battery system, assuming the electricity price remains or increases (which is very unlikely, as hydrogen and electricity are closely associated when hydrogen is renewably produced). But even with a 50% increase in diesel fuel costs and a 50% decrease in hydrogen costs, the diesel system shows a lower TAC.

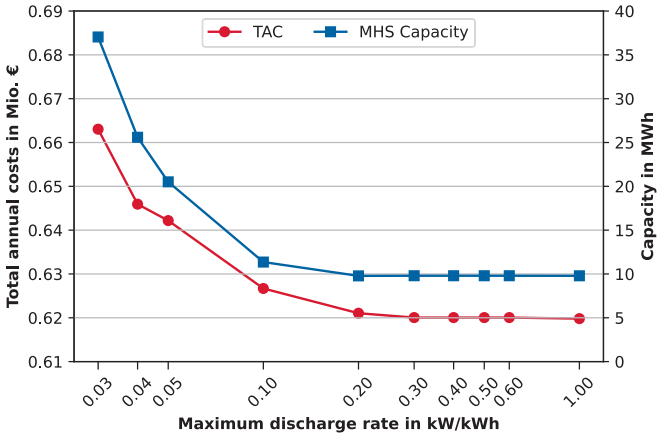

Fig. 16. Different maximum discharge rate for the metal hydride storage (TAC Total annual costs, MHS Metal hydride storage).

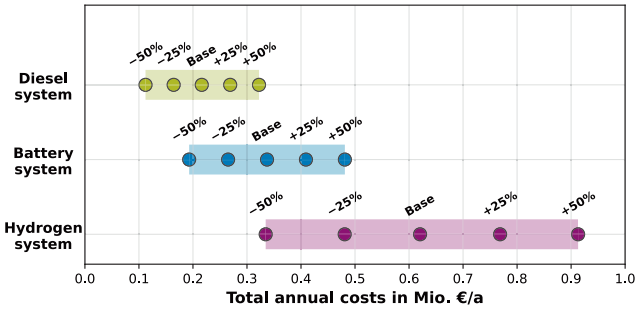

Fig. 17. Impact of changes in the cost of energy carriers (electricity, diesel fuel, and hydrogen) on total annual costs.

The results confirm the dominant effect of energy carrier costs on the TAC of individual systems and that reducing fuel costs through efficiency improvements, optimized driving behavior in real-world operation, or reduced energy carrier costs are the key levers for reducing the TAC. At the same time, the results also demonstrate their fundamental robustness: despite a moderate change in the systems, their basic ranking (hydrogen system most expensive, diesel system cheapest) remains unchanged. Only a concurrent and significant change in fuel costs that implies increasing and decreasing cost effects could change the economic viability of the systems, but such an event seems unlikely.

5. Final consideration

Defossilizing the shipping sector is a major challenge in the efforts to combat climate change. Besides the use of alternative GHG-neutral fuels in conventional combustion engines, especially for small and medium-sized ships, hydrogen-powered and battery-only propulsion systems might be a promising solution. For hydrogen-powered ships, metal hydride storage systems offer a feasible option for safely storing hydrogen at ambient conditions with a high volumetric energy density. In this paper, an optimization-based analysis is presented to investigate a possible design configuration and operational characteristics of a hydrogen-powered ship, compared with a conventional diesel-driven ship and a battery-only system. The focus here is on a short-distance ferry connection characterized by frequent cycles. The key results of this investigation are summarized below.

- The operational behavior of hydrogen-powered ships and diesel-driven vessels is widely comparable. For both options, small batteries can be implemented as a supporting energy source to shave peak energy demands.
- The most significant part (85%) of the usable “excess” heat generated by the fuel cell in the hydrogen-powered system can be used to unload hydrogen from the metal hydride storage tank. This is a major advantage compared to the diesel-powered system, where no demand for the waste heat released during the combustion of the diesel fuel is given; i.e., this use option for the waste heat released from the fuel cell enhances the overall efficiency of the hydrogen-powered system. Nevertheless, the lowest overall energy stored and released from a system is in the battery-only system, as direct electrification does not require high-loss conversion technologies (on the ferry).
- The needed volume for storages of the hydrogen system is only a third of the needed volume for the battery-only system, as long as no recharging at harbors during loading and unloading of goods is assumed.

- Looking only at the greenhouse gas (GHG) emissions from the fuels used within the operation modes, the battery-only system shows the lowest overall GHG emissions, followed by the hydrogen-powered system when "green" electricity is assumed. As electricity from the grid is still characterized by a certain share of fossil fuel energy, the emissions increase significantly within the hydrogen-powered system and the battery-only system if used. Compared to the hydrogen-powered system, the diesel-powered system shows 5 times higher GHG emissions, as most of the climate impact occurs during combustion.
- The total annual costs of all systems are clearly dominated by fuel costs; the CAPEX of the components play only a minor role, and only the battery in the battery-only system has a significant influence. The total annual costs are highest for the hydrogen system, followed by the battery system; the diesel system has the lowest annual costs, mainly due to its low diesel costs. Thus, by reducing the hydrogen fuel costs in the future (as it is most likely expected), a significant reduction in total annual costs can be achieved; however, it is unlikely that reducing the cost of the energy carrier alone will make such a system economically viable.
- If shore power is available, the total annual costs are hardly influenced. But storage capacities can be saved within the battery-only system.
- The uncertain data availability for the maximum discharge rate of the metal hydride storage does not affect the hydrogen-powered system's costs or storage capacity, as long as this is not assumed to be significantly lower than the value assumed in this work.

In summary, compared with a battery-only or diesel-powered propulsion system for such small-scale ships, the hydrogen-powered system has no technological implementation obstacles. This is particularly true in view of the driving profile discussed here, which requires a high number of cycles in combination with frequent acceleration processes. Particularly on smaller ships, where efficient use of space is crucial, volumetrically advantageous options such as metal hydride systems may be preferred over battery-only systems, especially if fuel cells and metal hydride materials are combined at a common temperature level to make efficient use of waste heat. The extent to which this can be implemented in technical terms, e.g., through process simulations, was not considered in this study and remains an open research question for future work. The specific tank design of a metal hydride storage system plays a particularly important role in this context. Future experimental studies could also help determine the actual cycle stability achievable with metal hydride storage tanks in real-world applications. Environmentally, both the hydrogen-powered system and the battery-only system can offer significant advantages over the diesel-powered system, as long as "green" electricity is used.

Funding

This work was funded by the German Federal Ministry of Research, Technology and Space (BMFTR) via the project HyPoKo (Grant no. 03SF0657C). Publishing fees supported by Funding Programme Open Access Publishing of Hamburg University of Technology (TUHH), Germany.

CRediT authorship contribution statement

Chris Drawer: Writing – original draft, Validation, Software, Methodology, Investigation, Formal analysis, Conceptualization. **Luka Bornemann:** Writing – review & editing, Validation, Software. **Martin Kaltschmitt:** Writing – review & editing, Supervision, Methodology.

Declaration of competing interest

The authors declare that they have no known competing financial interests or personal relationships that could have appeared to influence the work reported in this paper.

Appendix

Mathematical formulation

Details of the mathematical model are presented below. The input parameters are shown in Table A2. Additional information is provided in [23] and [36].

The investment costs for a component (C_c) with size (Q_c) are calculated with the economy of scale formula, based on investment costs (C_c^{ref}) for a reference size (Q_c^{ref}) to the power of a component-specific scale factor (M_c) (equation (A1)).

$$C_c = C_c^{ref}\left(\frac{Q_c}{Q_c^{ref}}\right)^{M_c}, \forall c \in \mathscr{C} \tag{A1}$$

Several components use an efficiency that is linked to their part load behavior with a set number (I_c) of support points for the relative input (λ_i^{in}) and output (λ_i^{out}) of a component (c). For each timestep, exactly one segment (i) is active, which is indicated by a binary variable ($\delta_{c,i}$), while the continuous variable ($l_{c,i}$) describes the relative power within an active segment. The slope for a segment is described via $\beta_{c,i}$ which is calculated from the neighboring support points. Degradation is neglected, meaning that efficiencies remain constant over time. As outlined in equation (A2), the input power ($\dot{Q}_c^{in}$) is expressed as a piecewise-linear function of the outgoing power ($\dot{Q}_c^{out}$) using these parameters for each component c.

$$\dot{Q}_c^{in} = \sum\nolimits_{i\in I_c}\left[\lambda_i^{in}\delta_{c,i}(t) + \beta_{c,i}\left(l_{c,i}(t) - \lambda_i^{out}\delta_{c,i}(t)\right)\right]\dot{Q}_c^{out}, \forall c \in \mathscr{C}, \forall t \in \mathscr{T} \tag{A2}$$

Equation (A3) defines the segment slopes.

$$\beta_{c,i} = \frac{\lambda_{i+1}^{in} - \lambda_i^{in}}{\lambda_{i+1}^{out} - \lambda_i^{out}}, \forall i = 1, \cdots, |I_c| - 1 \tag{A3}$$

For each storage ($s \in \mathscr{S}$), the state of charge definition for the following timestep ($SOC_{s,t+1,}$) includes the state of charge definition of the current timestep ($SOC_{s,t}$), the charge ($\dot{Q}_{s,t}^{in}$) and discharge power ($\dot{Q}_{s,t}^{out}$) multiplied by the respective charge (η_s^{charge}) and discharge ($\eta_s^{discharge}$) efficiencies, the self-

discharge of the storage (η_s^{self}) and the respective timestep length (Δt) (equation (A4)).

$$SOC_{s,t+1,} = SOC_{s,t}\left(1-\eta_s^{self}\Delta t\right) + \Delta t\left(\dot{Q}_{s,t}^{in}\eta_s^{charge} - \frac{\dot{Q}_{s,t}^{out}}{\eta_s^{discharge}}\right), \forall s \in \mathscr{S}, \forall t \in \mathscr{T} \quad (A4)$$

The state of charge is limited by a relative maximum state of charge (SOC_s^{max}) and a minimum state of charge (SOC_s^{min}), based on the storage capacity (Q_s) (equation (A5)).

$$SOC_s^{min}Q_s \le SOC_{s,t} \le SOC_s^{max}Q_s, \forall s \in \mathscr{S}, \forall t \in \mathscr{T} \quad (A5)$$

For the battery within the diesel- and hydrogen-powered systems, Equation (A6) shows that for the state of charge at the start of the time ($SOC_{s,t1}$) has to be on the same level as at the end of the time period ($SOC_{s,tn+1}$).

$$SOC_{s,t1,} = SOC_{s,tn+1}, \forall s \in \mathscr{S}^{Bat}, \forall t \in \mathscr{T} \quad (A6)$$

The relative minimum (α_c^{min}) and maximum (α_c^{max}) loads of the components output, dependent on the component size (Q_c) when turned on ($x_{c,t} = 1$; off: $x_{c,t} = 0$) is described in equation (A7).

$$\alpha_c^{min}Q_c x_{c,t} \le \dot{Q}_{c,t}^{out} \le \alpha_c^{max}Q_c x_{c,t}, \forall c \in \mathscr{C}, \forall t \in \mathscr{T} \quad (A7)$$

Table A1. Supporting points part-load behavior; part-load fraction inputs (λ_i^{in}) and outputs (λ_i^{out}).

Component	$\lambda_{i,1}^{in}$	$\lambda_{i,1}^{out}$	$\lambda_{i,2}^{in}$	$\lambda_{i,2}^{out}$	$\lambda_{i,3}^{in}$	$\lambda_{i,3}^{out}$	$\lambda_{i,4}^{in}$	$\lambda_{i,4}^{out}$	References
Fuel cell	0.1823	0.1514	0.5364	0.5670	0.7344	0.7665	1	1	[37]
Diesel engine	0.1219	0.1	0.4118	0.4	0.6220	0.65	1	1	[8]

Table A2. Techno-economic parameters (WACC Weighted Average Cost of Capital).

Component	Parameter	Value	Reference
PEM fuel cell	CAPEX [€/kW]	3,044	[38]
	Reference size [kW]	1	[38]
	Scale factor [-]	0.6889	[36]
	Lifetime [a]	14	[39]
	Maintenance factor [%/a]	3.8	[39]
	Electrical efficiency [-]	0.5	[39,40]
	Thermal efficiency [-]	0.3	[39]
Battery	CAPEX [€/kWh]	750	[41]
	Reference size [kW]	1	[41]
	Scale factor [-]	0.8382	[36]
	Lifetime [a]	15	[41]
	Maintenance factor [%/a]	2.2	[39]
	Charge / discharge efficiency [-]	0.9	[41]
	Charge / discharge max. [kW/kWh]	0.36	[42]
	Self-discharge [kW/kWh]	$4.2{\cdot}10^{-5}$	[42]
	Min. state of charge [-]	0	[36]
	Max. state of charge [-]	1	[36]
Metal hydride storage	CAPEX [€/kWh]	218	[43]
	Reference size [kW]	1	[43]
	Scale factor [-]	0.7509	[44]
	Lifetime [a]	30	[43]
	Maintenance factor [%/a]	2.0	[43]
	Reaction enthalpy FeTi [kJ/mol]	-24.6	[45]
	Charge / discharge efficiency [-]	1	Assumption
	Charge max. [kW/kWh]	0.75	[46]
	Discharge max. [kW/kWh]	0.38	Assumption based on [46,47]
	Self-discharge [kW/kWh]	0	Assumption
	Efficiency heat exchanger [-]	0.8	[48]
	Min. state of charge [-]	0.1	[49]
	Max. state of charge [-]	0.9	[49]
Diesel engine	CAPEX [€/kW]	590	[50]
	Reference size [kW]	1	Assumption
	Scale factor [-]	0.7	[51]
	Lifetime [a]	20	[50]
	Maintenance factor [%/a]	4.5	[20]
	Electrical efficiency [-]	0.44	[52,53]
	Thermal efficiency [-]	0.3	Assumption
	WACC [%]	8	[22]
	Inflation [%/a]	2	[22]

Fuel cost data

Table A3. Cost data and economic parameters.

Parameter	Value	References
Hydrogen price [€/kWh]	0.200	[54]
Electricity price [€/kWh]	0.180	[55]
Diesel price [€/kWh]	0.064	[56]

Emissions factors

The emission factors (Table A4) used to determine greenhouse gas emissions include not only emissions generated during use, but also those incurred in the provision of the corresponding energy source. A so-called "well-to-wheel" balance is assumed, i.e., from extraction to propulsion. Only diesel fuel causes emissions during operation (during combustion), accounting for the majority (83%) of total diesel-related emissions. The remaining 17% is released during diesel fuel production, e.g., in refineries [35]. Hydrogen and electricity do not cause emissions during operation, but emissions are generated during their production. In the case of hydrogen, the majority of emissions are caused by electricity generation (96%) [34]. Electricity generation, in turn, includes emissions from the combustion of fossil fuels (in the electricity mix) as well as emissions caused by renewable energies through the construction of photovoltaic systems, for example, which produce electricity per kWh.

Table A4. Greenhouse gas emission factors.

Fuel	*Emission factor [g CO_2-eq/kWh]*	*References*
Hydrogen (renewable energies)	*70*	[57]
Hydrogen (grid mix)	*510*	[57,58]
Electricity (renewable energies)	*42*	[57]
Electricity (grid mix)	*315*	[58]
Diesel	*317*	[59]

Data availability

Data will be made available on request.

References

[1] Li Z, Wang K, Liang H, Wang Y, Ma R, Cao J, et al. Marine alternative fuels for shipping decarbonization: Technologies, applications and challenges. Energ Conver Manage 2025;329:119641. https://doi.org/10.1016/j.enconman.2025.119641.

[2] Tomos BAD, Stamford L, Welfle A, Larkin A. Decarbonising international shipping – a life cycle perspective on alternative fuel options. Energ Conver Manage 2024; 299:117848. https://doi.org/10.1016/j.enconman.2023.117848.

[3] Lee H, Lee J, Roh G, Lee S, Choung C, Kang H. Comparative Life Cycle Assessments and Economic analyses of Alternative Marine Fuels: Insights for Practical strategies. Sustainability 2024;16:2114. https://doi.org/10.3390/su16052114.

[4] Bullerdiek N, Neuling U, Kaltschmitt M, editors. Powerfuels: Status and Prospects. Cham: Springer Nature Switzerland; 2025. https://doi.org/10.1007/978-3-031-62411-7.

[5] Ganji M, Gheibi M, Aldaghi A, Dhoska K, Vito S, Atari S, et al. Comprehensive Study on Hydrogen Production for Sustainable Transportation Planning: Strategic, Techno-Economic, and Environmental Impacts. Hydrogen 2025;6:24. https://doi.org/10.3390/hydrogen6020024.

[6] Le P-A, Trung VD, Nguyen PL, Bac Phung TV, Natsuki J, Natsuki T. The current status of hydrogen energy: an overview. RSC Adv 2023;13:28262–87. https://doi.org/10.1039/D3RA05158G.

[7] Perna A, Jannelli E, Di Micco S, Romano F, Minutillo M. Designing, sizing and economic feasibility of a green hydrogen supply chain for maritime transportation. Energ Conver Manage 2023;278:116702. https://doi.org/10.1016/j.enconman.2023.116702.

[8] Dall'Armi C, Micheli D, Taccani R. Comparison of different plant layouts and fuel storage solutions for fuel cells utilization on a small ferry. International Journal of Hydrogen Energy 2021;46:13878–97.

[9] Drawer C, Lange J, Kaltschmitt M. Metal hydrides for hydrogen storage – Identification and evaluation of stationary and transportation applications. J Storage Mater 2024;77:109988. https://doi.org/10.1016/j.est.2023.109988.

[10] Kim S, Oh S, Kang S. Techno-economic assessment of liquefied hydrogen tanker ships utilizing various propulsion systems. Energ Conver Manage 2025;336: 119895. https://doi.org/10.1016/j.enconman.2025.119895.

[11] Ghorbani B, Zendehboudi S, Alizadeh Afrouzi Z, Saady NMC. Optimized hydrogen boil-off gas re-liquefaction process for marine transport: Exergy, economic, environmental, and uncertainty perspectives. Energy 2025;338:138605. https://doi.org/10.1016/j.energy.2025.138605.

[12] Abetz C, Georgopanos P, Pistidda C, Klassen T, Abetz V. Reactive Hydride Composite Confined in a Polymer Matrix: New Insights into the Desorption and Absorption of Hydrogen in a Storage Material with High Cycling Stability. Adv Materials Technologies 2022;7:2101584. https://doi.org/10.1002/admt.202101584.

[13] Cavo M, Gadducci E, Rattazzi D, Rivarolo M, Magistri L. Dynamic analysis of PEM fuel cells and metal hydrides on a zero-emission ship: a model-based approach. Int J Hydrogen Energy 2021;46:32630–44. https://doi.org/10.1016/j.ijhydene.2021.07.104.

[14] Liu Y, Liu S, Li G, Gao X. Strategy of Enhancing the Volumetric Energy Density for Lithium–Sulfur Batteries. Adv Mater 2021;33:2003955. https://doi.org/10.1002/adma.202003955.

[15] Klopčič N, Grimmer I, Winkler F, Sartory M, Trattner A. A review on metal hydride materials for hydrogen storage. J Storage Mater 2023;72:108456. https://doi.org/10.1016/j.est.2023.108456.

[16] Katumwesigye A, Schwartz H, Gustafsson M, Hellström M. A comparative technoeconomic and life cycle assessment of a fully battery-electric ROPAX ferry. J Clean Prod 2025;534:146935. https://doi.org/10.1016/j.jclepro.2025.146935.

[17] Moon HS, Park WY, Hendrickson T, Phadke A, Popovich N. Exploring the cost and emissions impacts, feasibility and scalability of battery electric ships. Nat Energy 2024;10:41–54. https://doi.org/10.1038/s41560-024-01655-y.

[18] Al-Falahi MDA, Coleiro J, Jayasinghe SDG, Enshaei H, Garaniya V, Baguley C, et al. In: Techno-Economic Feasibility Study of Battery- Powered Ferries. Singapore, Singapore: IEEE; 2018. p. 1–7. https://doi.org/10.1109/SPEC.2018.8636010.

[19] Cha M, Enshaei H, Nguyen H, Jayasinghe SG. Optimal sizing and evaluation of efficient fuel cell utilization for fuel cell battery hybrid electric ferry. Energ Conver Manage 2024;315:118723. https://doi.org/10.1016/j.enconman.2024.118723.

[20] Kistner L, Bensmann A, Minke C, Hanke-Rauschenbach R. Comprehensive techno-economic assessment of power technologies and synthetic fuels under discussion for ship applications. Renew Sustain Energy Rev 2023;183:113459. https://doi.org/10.1016/j.rser.2023.113459.

[21] Van Sickle E, Ralli P, Pratt JW, Klebanoff LE. MV Sea Change: the first commercial 100% hydrogen fuel cell passenger ferry in the world. Int J Hydrogen Energy 2025; 105:389–404. https://doi.org/10.1016/j.ijhydene.2025.01.040.

[22] Sens L, Piguel Y, Neuling U, Timmerberg S, Wilbrand K, Kaltschmitt M. Cost minimized hydrogen from solar and wind – production and supply in the European catchment area. Energ Conver Manage 2022;265:115742. https://doi.org/10.1016/j.enconman.2022.115742.

[23] Sass S, Faulwasser T, Hollermann DE, Kappatou CD, Sauer D, Schütz T, et al. Model compendium, data, and optimization benchmarks for sector-coupled energy systems. Comput Chem Eng 2020;135:106760. https://doi.org/10.1016/j.compchemeng.2020.106760.

[24] Commission Delegated Regulation (EU) 2023/1184 of 10 February 2023 supplementing Directive (EU) 2018/2001 of the European Parliament and of the

Council by establishing a Union methodology setting out detailed rules for the production of renewable liquid and gaseous transport fuels of non-biological origin. 2023.
[25] MarineTraffic.com. MarineTraffic: Global Ship Tracking Intelligence | AIS Marine Traffic 2025. https://www.marinetraffic.com/en/ais/home/centerx:-12.0/centery:25.0/zoom:4 (accessed December 15, 2025).
[26] Damian SE, Wong LA, Shareef H, Ramachandaramurthy VK, Chan CK, Moh TSY, et al. Review on the challenges of hybrid propulsion system in marine transport system. J Storage Mater 2022;56:105983. https://doi.org/10.1016/j.est.2022.105983.
[27] Jeong B, Oguz E, Wang H, Zhou P. Multi-criteria decision-making for marine propulsion: Hybrid, diesel electric and diesel mechanical systems from cost-environment-risk perspectives. Appl Energy 2018;230:1065–81. https://doi.org/10.1016/j.apenergy.2018.09.074.
[28] Shanshal A. Charging hybrid is the future for ferries. 2022.
[29] Al-Falahi MDA, Nimma KS, Jayasinghe SDG, Enshaei H, Guerrero JM. Power management optimization of hybrid power systems in electric ferries. Energ Conver Manage 2018;172:50–66. https://doi.org/10.1016/j.enconman.2018.07.012.
[30] Schoenebeck G von. Hybridfähre: Abgasfrei und leise beim Aus- und Einlaufen. ingenieur.de - Jobbörse und Nachrichtenportal für Ingenieure 2016. https://www.ingenieur.de/technik/fachbereiche/verkehr/hybridfaehre-abgasfrei-leise-aus-einlaufen/ (accessed October 14, 2025).
[31] Transient Performance Specifications for Diesel Generator Sets | Cat | Caterpillar. Https://WwwCatCom/en_US/by-Industry/Electric-Power/Articles/White-Papers/Transient-Performance-Specifications-for-Diesel-Generator-SetsHtml n.d. https://www.cat.com/en_US/by-industry/electric-power/Articles/White-papers/transient-performance-specifications-for-diesel-generator-sets.html (accessed October 14, 2025).
[32] Chandran M, Palaniswamy K, Karthik Babu NB, Das O. A study of the influence of current ramp rate on the performance of polymer electrolyte membrane fuel cell. Sci Rep 2022;12:21888. https://doi.org/10.1038/s41598-022-25037-0.
[33] Zhou K, Wu Y, Wu X, Sun Y, Teng D, Liu Y. Research and Development Review of Power Converter Topologies and Control Technology for Electric Vehicle Fast-Charging Systems. Electronics 2023;12:1581. https://doi.org/10.3390/electronics12071581.
[34] Bareiß K, De La Rua C, Möckl M, Hamacher T. Life cycle assessment of hydrogen from proton exchange membrane water electrolysis in future energy systems. Appl Energy 2019;237:862–72. https://doi.org/10.1016/j.apenergy.2019.01.001.
[35] Edwards R, Mahieu V, Griesemann J-C, Larivé J-F, Rickeard DJ. Well-to-Wheels Analysis of Future Automotive Fuels and Powertrains in the European Context, Toulouse, France: 2004, p. 2004-01–1924. https://doi.org/10.4271/2004-01-1924.
[36] Bornemann L, Lange J, Kaltschmitt M. A rigorous optimization method for long-term multi-stage investment planning: Integration of hydrogen into a decentralized multi-energy system. Energy Rep 2025;13:117–39. https://doi.org/10.1016/j.egyr.2024.11.079.
[37] Gabrielli P, Gazzani M, Mazzotti M. Electrochemical conversion technologies for optimal design of decentralized multi-energy systems: Modeling framework and technology assessment. Appl Energy 2018;221:557–75. https://doi.org/10.1016/j.apenergy.2018.03.149.
[38] Li N, Lukszo Z, Schmitz J. An approach for sizing a PV–battery–electrolyzer–fuel cell energy system: a case study at a field lab. Renew Sustain Energy Rev 2023;181:113308. https://doi.org/10.1016/j.rser.2023.113308.
[39] Petkov I, Gabrielli P. Power-to-hydrogen as seasonal energy storage: an uncertainty analysis for optimal design of low-carbon multi-energy systems. Appl Energy 2020;274:115197. https://doi.org/10.1016/j.apenergy.2020.115197.
[40] Cigolotti V, Genovese M, Fragiacomo P. Comprehensive Review on fuel Cell Technology for Stationary Applications as Sustainable and Efficient Poly-Generation Energy Systems. Energies 2021;14:4963. https://doi.org/10.3390/en14164963.
[41] Kost C, Müller P, Schweiger JS, Fluri V, Thomson J. Levelized Cost of Electricity - Renewable Energy Technologies 2024.
[42] Baumgärtner N, Shu D, Bahl B, Hennen M, Hollermann DE, Bardow A. DeLoop: Decomposition-based long-term operational optimization of energy systems with time-coupling constraints. Energy 2020;198:117272. https://doi.org/10.1016/j.energy.2020.117272.
[43] Danebergs J, Deledda S. Can hydrogen storage in metal hydrides be economically competitive with compressed and liquid hydrogen storage? a techno-economical perspective for the maritime sector. Int J Hydrogen Energy 2024;50:1040–54. https://doi.org/10.1016/j.ijhydene.2023.08.313.
[44] Testi M, Prattico L, Ragaglia D. HyCARE Hydrogen CArrier for Renewable Energy Storage -. Techno-Economic Analysis 2023.
[45] Shang Y, Liu S, Liang Z, Pyczak F, Lei Z, Heidenreich T, et al. Developing sustainable FeTi alloys for hydrogen storage by recycling. Commun Mater 2022;3. https://doi.org/10.1038/s43246-022-00324-5.
[46] Krastev V, Bella G, Falcucci G, Bartolucci L, Cordiner S, Mulone V. Power Vs. Capacity Performances of Thermally Integrated MH-PCM Hydrogen Storage Solutions: Current Status and Development Perspectives. 36th International Conference on Efficiency, Cost, Optimization, Simulation and Environmental Impact of Energy Systems (ECOS 2023), Las Palmas De Gran Canaria, Spain: ECOS 2023; 2023, p. 2183–93. https://doi.org/10.52202/069564-0197.
[47] Wang C-S, Brinkerhoff J. Predicting hydrogen adsorption and desorption rates in cylindrical metal hydride beds: Empirical correlations and machine learning. Int J Hydrogen Energy 2021;46:24256–70. https://doi.org/10.1016/j.ijhydene.2021.05.007.
[48] Kumar S, Sharma R, Srinivasa Murthy S, Dutta P, He W, Wang J. Thermal analysis and optimization of stand-alone microgrids with metal hydride based hydrogen storage. Sustainable Energy Technol Assess 2022;52:102043. https://doi.org/10.1016/j.seta.2022.102043.
[49] Valverde L, Bordons C, Rosa F. Integration of fuel Cell Technologies in Renewable-Energy-Based Microgrids Optimizing Operational Costs and Durability. IEEE Trans Ind Electron 2016;63:167–77. https://doi.org/10.1109/TIE.2015.2465355.
[50] Ahluwalia RK, Rail LAN. Aviation, and Maritime Metrics 2021.
[51] James R, Turner M, Samaei A. Quality guidelines for Energy System Studies: Capital cost Scaling Methodology. Revision 3 Reports and Prior 2019. https://doi.org/10.2172/1567182.
[52] Pyrhönen DJ, Lindh DP. Design of marine generators for alternative diesel-electric power systems 2011.
[53] Vedran M, Božica SŽ, Jasna P-O. MARINE SLOW SPEED TWO-STROKE DIESEL ENGINE - NUMERICAL ANALYSIS OF EFFICIENCIES AND IMPORTANT OPERATING PARAMETERS 2017.
[54] Cost of hydrogen production | European Hydrogen Observatory n.d. https://observatory.clean-hydrogen.europa.eu/hydrogen-landscape/production-trade-and-cost/cost-hydrogen-production (accessed October 14, 2025).
[55] BDEW Bundesverband der Energie- und Wasserwirtschaft e.V. BDEW-Strompreisanalyse Mai 2025 2025. https://www.bdew.de/service/daten-und-grafiken/bdew-strompreisanalyse/ (accessed June 4, 2025).
[56] Hamburg Bunker Fuel Prices Today, IFO 380, IFO 180, MGO Prices per Ton. OilMonster n.d. https://www.oilmonster.com/bunker-fuel-prices/west-northern-europe/hamburg/130 (accessed October 14, 2025).
[57] Drawer C, Rödl A, Kaltschmitt M. Life cycle assessment of construction and driving operation of a hydrogen-powered truck built from a used diesel truck. Transp Res Interdiscip Perspect 2024;24:101020. https://doi.org/10.1016/j.trip.2024.101020.
[58] Lewicki P. Strom- und Wärmeversorgung in Zahlen. Umweltbundesamt 2013. https://www.umweltbundesamt.de/themen/klima-energie/energieversorgung/strom-waermeversorgung-in-zahlen (accessed October 14, 2025).
[59] „Wie viel CO2 steckt in einem Liter Benzin?“. Helmholtz-Gemeinschaft Deutscher Forschungszentren 2020. https://www.helmholtz.de/newsroom/artikel/wie-viel-co2-steckt-in-einem-liter-benzin/ (accessed October 14, 2025).